Simple design method for partially prestressed concrete structures

Autor(en): **Braam, Cornelis R. / Frénay, Jerome W.**

Objekttyp: **Article**

Zeitschrift: **IABSE proceedings = Mémoires AIPC = IVBH Abhandlungen**

Band (Jahr): **13 (1989)**

Heft P-136: **Simple design method for partially prestressed concrete structures**

PDF erstellt am: **22.07.2024**

Persistenter Link: https://doi.org/10.5169/seals-41971

Simple Design Method for Partially Prestressed Concrete Structures

Méthode simple de calcul pour des structures en béton partiellement précontraint

Einfache Rechenmethode für den Entwurf von teilweise vorgespannten Betonkonstruktionen

Cornelis R. BRAAM
Civil Engineer
Delft Univ. of Techn. (DUT)
Delft, The Netherlands

Jerome W. Frénay
Civil Engineer
Inst. of Agricultural Eng. (IMAG)
Wageningen, The Netherlands

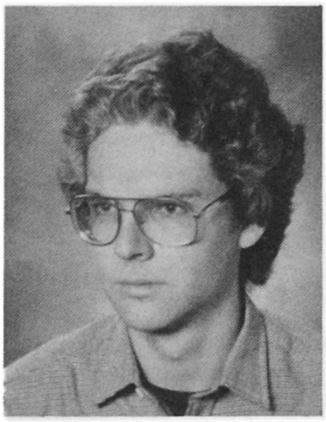

Cornelis R. Braam, born 1961, graduated as Civil Engineer M. Sc. at the Delft University of Technology. In 1985 he joined the research group of the Stevinlaboratory of the Faculty of Civil Engineering (DUT).

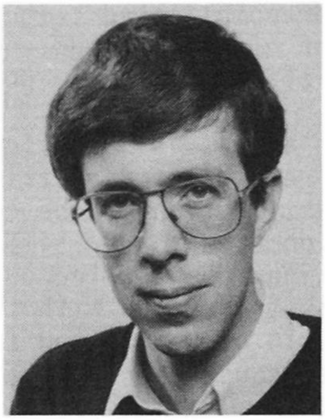

Jerome W. Frénay, born 1956, is senior researcher at the structures department of IMAG in Wageningen. He received his M. Sc. Civil Engineering degree at the Delft University of Technology where he joined the concrete structures group from 1982-1988.

SUMMARY

This paper presents an overview of a simple calculation method for concrete structures provided with a combination of reinforcing steel bars and post-tensioned prestressing. The approach chosen relates closely to present theoretical modelling techniques aimed at a satisfactory approximation of the actual structural concrete behaviour. The proposed method is illustrated by means of two statically indeterminate concrete structures; a rectangular girder for a warehouse and a box-girder bridge used for a motorway.

RÉSUMÉ

Cette publication donne un aperçu d'une méthode de calcul simple pour des structures en béton pourvues d'une combinaison d'armature en acier ordinaire et de câbles de post-contrainte. L'approche choisie a le but d'obtenir une approximation satisfaisante pour le comportement du béton structural. La méthode est illustrée pour deux structures hyperstatiques en béton, notamment une poutre rectangulaire pour un dépôt et une poutre en utilisée pour un pont d'autoroute.

ZUSAMMENFASSUNG

In diesem Aufsatz wird eine einfache Rechenmethode für teilweise vorgespannten Beton vorgestellt. Die gewählte Vorgehensweise schliesst an moderne Rechentechniken an, die zum Ziel haben, das Verhalten von Betonkonstruktionen so wirklichkeitsnah wie möglich zu beschreiben. Die vorgeschlagene Methode wird an zwei Beispielen illustriert: an einem rechteckigen Träger für ein Lagerhaus und an einer Hohlkastenbrücke für eine Autobahn.

1. INTRODUCTION

The design and behaviour of partially prestressed concrete structures have been discussed in the literature for many years [1]. Several researchers proposed computational methods applicable for the combined action of both reinforcing and prestressing steel [2-7]. It is endeavoured to model reinforced concrete as well as fully prestressed concrete structures by means of one clear and unequivocal computational approach. However, there is still a lack of sufficient theoretical and experimental evidence.

In spite of the extensive research, the number of partially prestressed concrete applications in The Netherlands is limited. Today, a similar situation exists in many other European countries with the exception of Switzerland [33]. There are technical and economic factors which may hinder these new developments. It is thought that the structural engineer and the building-authorities both have a lot of questions, such as:

- Are cracks in concrete allowed if crossed by prestressing steel?;
- How should rather complicated calculation methods be coped with?;
- Which combination of reinforcing and prestressing steel should be chosen and how does it affect the building-costs?

Another limitation arises as specific national or international code rules hardly exist with respect to partially prestressed concrete. Thus, there are no criteria for verification of the computational results. Therefore, this paper pays attention to a rather simple calculation method based on recent theoretical investigations carried out at the Delft University of Technology. The approach proposed links up with the international scientific progress achieved in the field of reinforced and fully prestressed concrete. It should also contribute to reduce the uncertainty and confusion about partially prestressed concrete.

First, the basic assumptions of the method are briefly dealt with in chapter 2. Next, two practical structural applications are presented in chapters 3 and 4. The first example concerns a statically indeterminate beam which is part of a warehouse. Emphasis lies on the types of reinforcement chosen, the predicted crack widths, the shear transfer and the structural safety. The second problem refers to some other aspects, for instance the steel stress variation of the reinforcement in case of traffic loading applied on a system of box-girders in partially prestressed concrete. The computational results are compared with a finite element analysis admitting physical non-linear modelling techniques. Finally, a few conclusions are summarized in chapter 5.

2. BASIC ASSUMPTIONS

2.1 Distribution of forces

The cross-sectional area of the reinforcement in the various cross-sections is calculated on the basis of the distribution of forces, obtained using the theory of elasticity. This implies that no redistribution of forces is adopted in the ultimate limit state.

2.2 Equivalent loading by prestressing

By prestressing, a system of equivalent forces is applied on the structure: these forces are either concentrated (anchorages) or distributed (pressure by curved cables). The level of effective prestressing includes stress losses due to friction and time-dependent material behaviour, such as creep and shrinkage of the concrete and relaxation of the prestressing steel. It is assumed that shrinkage and creep develop unrestrained which means that they are not affected by the embedded reinforcement.

2.3 Cracking behaviour

The effect of prestressing should be taken into account in the calculation of the cracking moment M_{cr}, the crack spacing and the crack width. The predicted crack width provides a criterion for the distinction of three types of structural concrete [5,32], see figure 1. They may also be characterized by the degree of prestressing K, defined as:

$$K = M_o / M_{max} \qquad [-] \qquad (1)$$

where M_o is the decompression moment for which the concrete stress $\sigma_{co} = 0$ at the outer fibre of the structure. M_{max} is the maximum bending moment caused by external loading at the serviceability limit state. Cracks are expected for $K < 1.0$ unless $\sigma_c < f_{ct}$ at the outer fibres.

In case of partial prestressing, the value of M_{cr} can easily be calculated, if the effect of prestressing is represented by an axial force P_∞ and a bending moment $M_{p\infty}$ (see figures 2a-b).

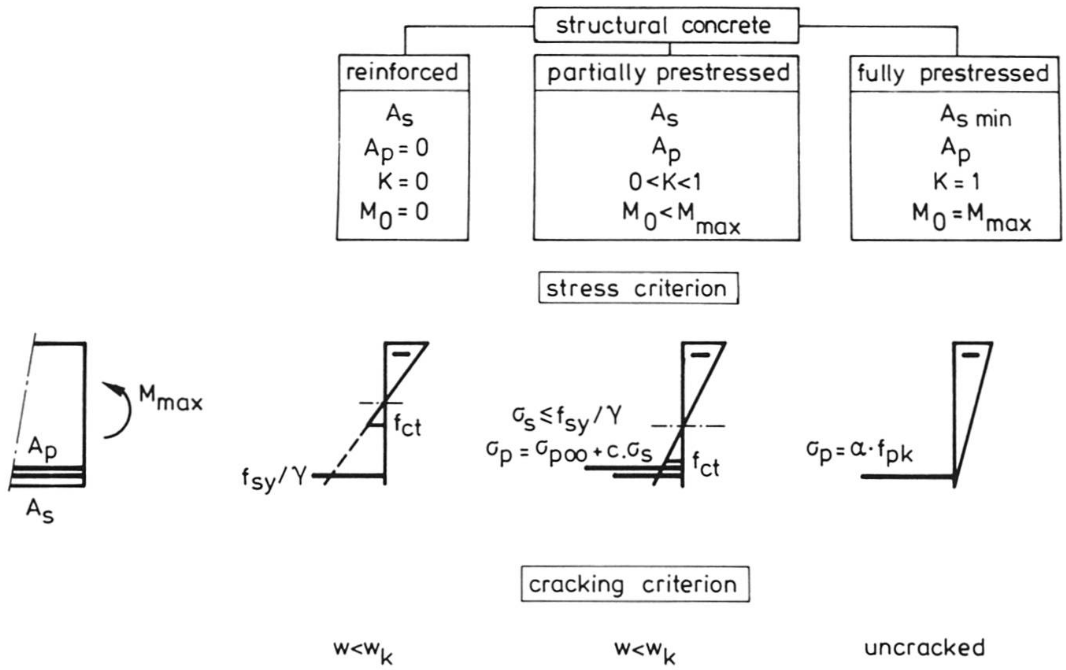

Fig. 1 Types of structural concrete at the serviceability limit state.

This procedure basically corresponds to the approach applied for reinforced concrete. Either the pure tensile strength or the flexural tensile strength is used as a cracking criterion for concrete: $f_{ct,fl}$ depends on the strain gradient over the structure. It means that cracking is related to the structural geometry. In [8] a formula is given for both types of tensile strengths:

$$\frac{f_{ct,fl}}{f_{ct}} = (0.6 + 0.4(2h_t)^{-0.25}) \qquad \geq 1 \qquad [-] \qquad (2)$$

where h_t denotes the height of the tension zone in m. The crack width is controlled by the reinforcement crossing the crack plane. Generally, the bond stresses developed between concrete and prestressing steel are lower than those between concrete and reinforcing steel. Therefore, the increase of the stress in the prestressing steel upon cracking is lower than the increase of the stress in the reinforcing steel. This is considered using the relation:

$$\Delta\sigma_{p,cr} = c.\Delta\sigma_{s,cr} \qquad (c < 1) \qquad [MPa] \qquad (3)$$

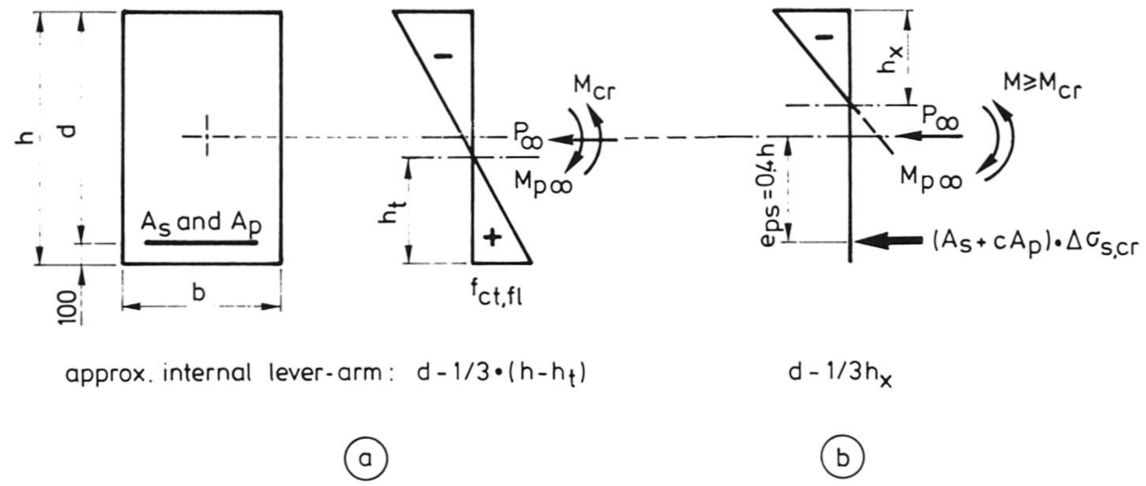

Fig. 2 Stress diagrams and internal forces (a) at and (b) after cracking.

Next, the crack spacings and widths are found by means of existing theoretical models [11,12], provided that the concrete cover is at least 1.5-2 times the largest bar diameter used.
National design codes [8,13] usually offer empirical relations for crack widths and spacings [14,15]. The field of application is often limited to reinforced concrete. Recently, several authors have developed extensions of existing theories to partially prestressed concrete [9,10,16].

2.4 Bending moment

The bending moment at the ultimate limit state follows from the static system. Thus $M^* = \gamma.M_{max}$ where γ denotes the structural safety factor including material as well as loading uncertainties. M^* should be obtained by the ultimate bending moment M_u of the cross-section. This bending moment is derived from simple equations of equilibrium, see figure 3. A factor $\gamma = 1.7$ is adopted according to the Dutch design code [19].

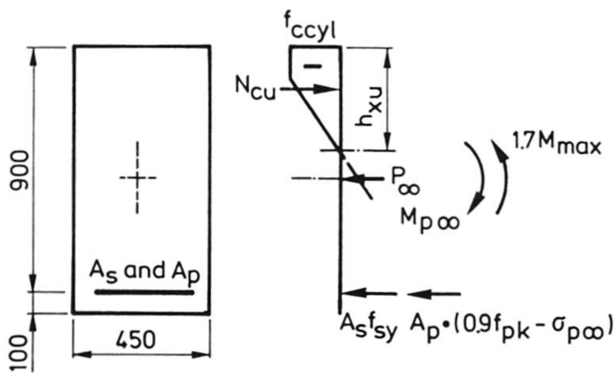

Fig. 3 Bending failure: stress diagram and internal forces.

As shown, the prestressing steel is simply considered as a type of reinforcement with an adapted yield stress. The effects of the equivalent loading by prestressing are all entered into the calculations. It is preferred to use at least a minimum amount of reinforcing steel in each cross-section (see figure 4) so that a distributed crack pattern and a sufficiently 'tough' structural behaviour at failure are ensured.

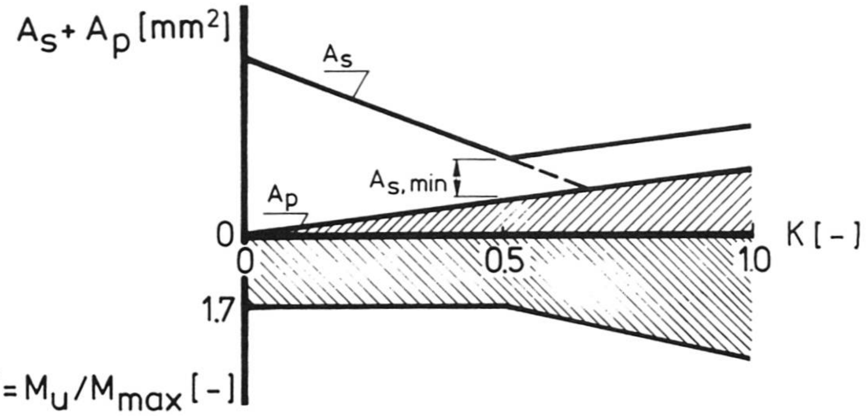

Fig. 4 Reinforcement ratio and structural safety factor, both as a function of the degree of prestressing.

2.5 Shear force

The distribution of internal forces again results from a linear-elastic analysis. The shear transfer consists of three components [31,35]:

- transfer by the concrete compression zone including the effect of the centric prestressing force;
- component of the vertical stirrups derived by means of the truss analogy;
- the effect of the equivalent loading exerted by the curved prestressing tendons.

The last-mentioned component may only be added if the tension zone is locally uncracked. If cracking occurs nevertheless, then the tensile capacity of this zone should conform to the following relations [17,18]:

$$A_s \cdot f_{sy} + A_p \cdot f_{pk} \geq V_d \qquad [N] \qquad (4a)$$

and:

$$A_s \cdot f_{sy} \geq V_d/2 \qquad [N] \qquad (4b)$$

These formulae are virtually inherent to the use of prestressing as an equivalent loading. Eq. (4b) refers to a distributed crack pattern, ensuring a reliable and durable structural design.

3. DESIGN OF A STATICALLY INDETERMINATE GIRDER IN PARTIALLY PRESTRESSED CONCRETE

3.1 Introduction

The calculation method presented in chapter 2 is now illustrated by means of a continuous girder with a rectangular cross-section chosen to simplify the computations of this example. See figures 5a-b. The girder is part of a warehouse and it supports a system of pre-fabricated slabs. The beam and the columns are monolithically connected. The bending stiffness of these columns may be neglected for the design of the beam. Due to the geometry of the building the

maximum height of the beam is restricted to 1000mm.
The characteristic (γ = 1.0) distributed loading amounts to:
q_p = 27 kN/m (dead load of girder and slabs)
q_q = 64 kN/m (live load on slab: approx. 12 kN/m^2)

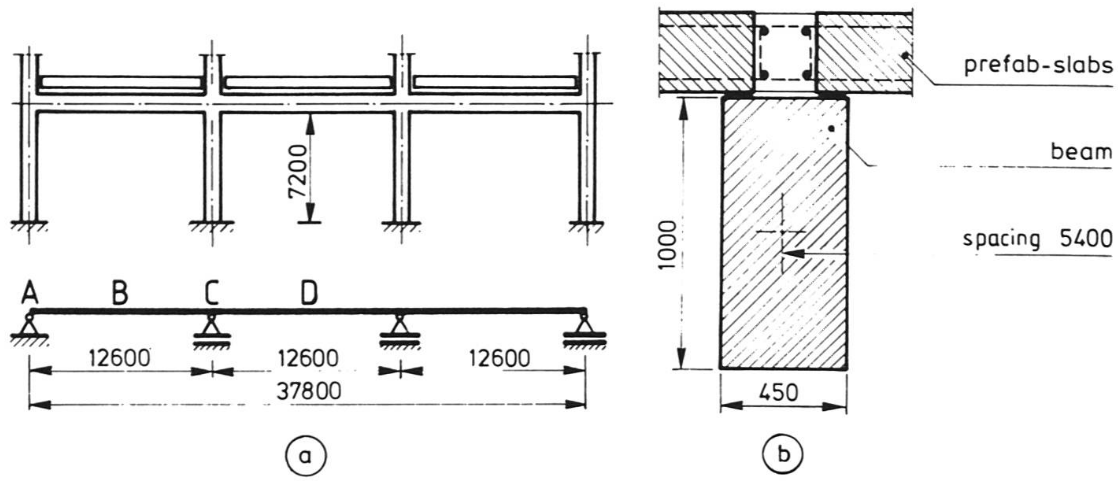

Fig. 5 Continuous girder: (a) side view and (b) cross-section.

A safety factor γ = 1.7 is used for all the loadings [19]. If the live load does not act on the full length of the girder, then it is reduced with 25%, so that a more realistic approximation of the actual load application is achieved The distribution of extreme values of the bending moment and the shear loading are presented in figure 6.

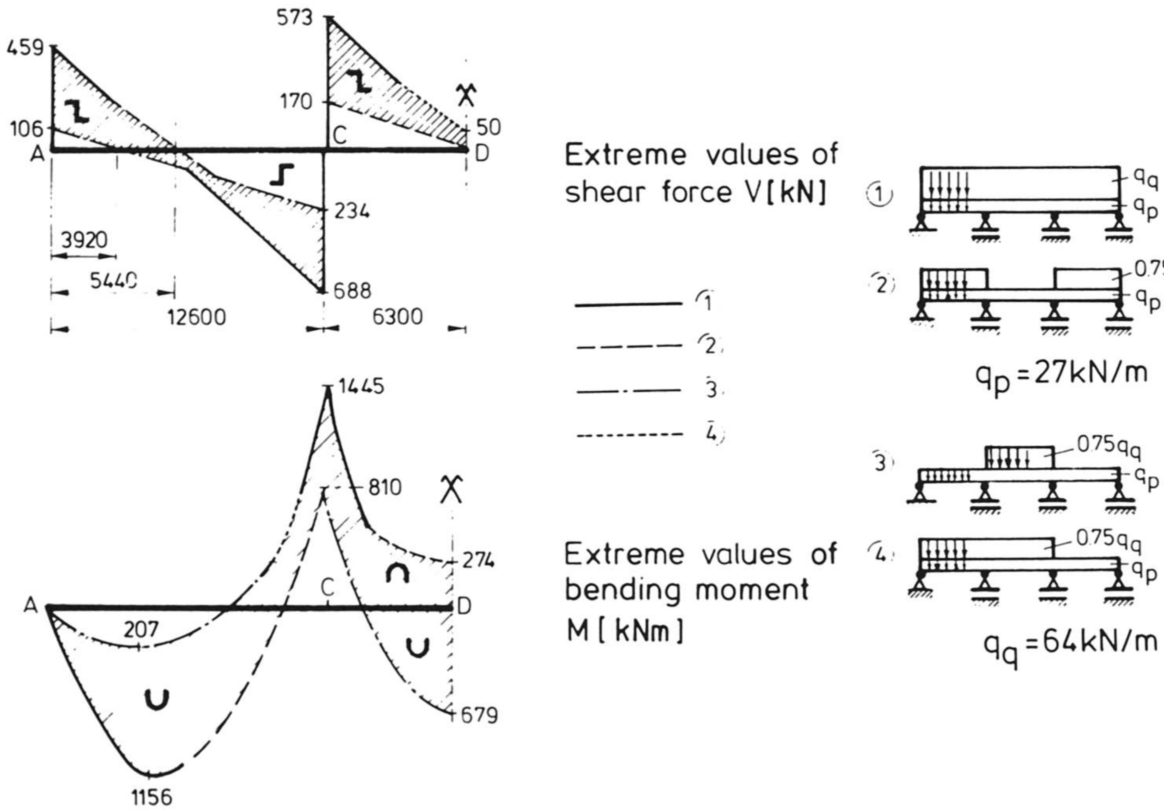

Fig. 6 Bending moment and shear force distribution: extreme values are indicated for γ = 1.0.

Additional information about the materials used is given below:

Concrete: normal-strength gravel concrete is used; compressive strength f_{cck}= 35 MPa; f_{ccylk}= 28 MPa; direct tensile strength $f_{ctk,0}$= 2.5 MPa.

The stress-strain diagram has a bi-linear shape, see figure 7.

Reinforcing steel: yield stress f_{sy}= 500 MPa, ribbed steel bars are used.

Prestressing steel: f_{pk}= 1860 MPa; effective prestress $\sigma_{p\infty} \leq 0.65 f_{pk}$.

$\sigma_{po} \leq 0.75 f_{pk}$ immediately after removal of the hydraulic prestressing jack.

The concrete cover is c_s= 40mm for the longitudinal steel bars and c_p= 50mm for the prestressing ducts. In case of reinforced concrete the 95% upper-bound characteristic crack width is restricted to w_k= 0.30mm for rather humid environmental conditions (70-80% RH). If supplementary prestressing steel is used, then w_k= 0.20mm is proposed [20].

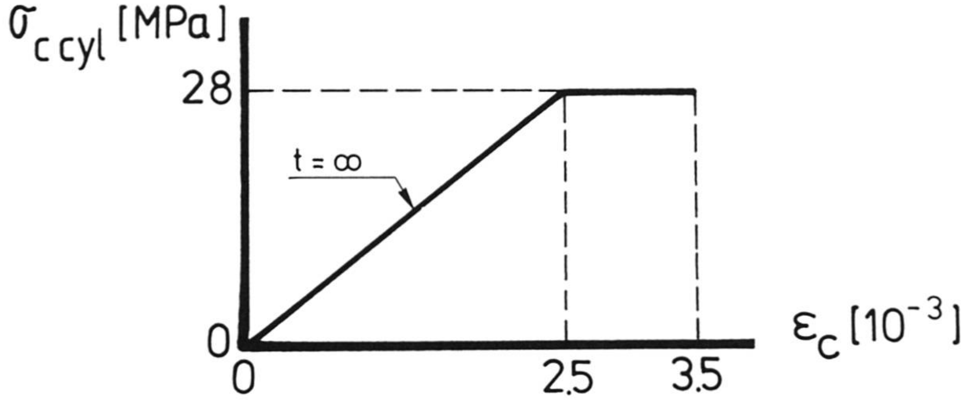

Fig. 7 Assumed stress-strain diagram for concrete in compression.

3.2 Reinforced concrete girder

The Dutch design code for concrete [19] allows a maximum reinforcement ratio for each cross-section which is equivalent to a sufficiently large rotational capacity of the complete structure. This condition can be easily transformed into a minimum steel strain $\epsilon_s = 1.5\epsilon_{sy}$ before failure of the concrete compression zone should occur.

In case of a 900mm effective depth of the beam the ultimate bending moment when applying the maximum reinforcement ratio is $M_u = 2700.10^6$ Nmm. Now the predicted structural safety of cross-section C yields:

$$\gamma = \frac{2700}{1445} = 1.87 > 1.70 \qquad [-] \qquad (5)$$

Table 1 shows however that fairly high amounts of steel are needed for γ = 1.7. In general ρ_d= 0.8-1.2% is economic for reinforced concrete beams with a rectangular cross-section.

Table 1 Reinforcement chosen for four cross-sections.

cross-section	A_s	ρ_d [%]
B	10 ϕ 25mm	1.21
C	14 "	1.70
D (◡)	6 "	0.73
D (⌒)	3 "	0.36

The drafts of both the CEB-FIP model code [8] and the Eurocode [13] were used to calculate the crack widths. The results showed that $w_k \leq 0.30$mm for all the cases considered. These crack widths agreed closely with a supplementary analysis based on theoretical models, such as presented in [11]. Some deviations occurred for the top bars, probably because the crack width formulas chosen in the codes do not distinguish between upper and lower bars. It should be realized that this position may strongly affect the bond characteristics of the embedded bars. Vertically placed closed stirrups are applied of a 12mm diameter at a minimum spacing of 110mm located at the left-hand side of cross-section C.

3.3 Girder in fully prestressed concrete

Here, the same type of girder is designed so that the degree of prestressing K = 1. The schematic location of the prestressing ducts and the cable eccentricities are presented in figure 8a. The cable was stressed at both end blocks of the beam. After the prestress losses due to friction along the tendon profile and due to time-dependent material behaviour are quantified, the equivalent prestress loadings are found, see figure 8b.The level of prestressing mainly depends on the permissible compressive and tensile stresses of the concrete related to the serviceability limit state. A fully prestressed girder could not be achieved, even if the position of the cable was systematically changed, without the application of a higher concrete grade. A rather good approximation was found for:

- $e_1 = e_2 = e_3 = 400$mm;

- $R_0 = 5000$mm; $R_1 = 31100$mm; $R_2 = 19800$mm and $P_0 = 2700.10^3$ N.

Three prestressing elements are needed of six 12.7mm (1/2 inch) diameter strands each, thus $A_p \simeq 3*600 = 1800$ mm². The duct diameter is 50/55mm. Due to the 'secondary moment' the line of thrust is situated 85mm above the centre line of the tendon profile at cross-section C.

3.4 Girder in partially prestressed concrete

Partially prestressed concrete offers an opportunity for the engineer to choose any combination of prestressing and reinforcing steel adapted to the specific structural system. However, each design should satisfy the requirements given for the serviceability limit state as well as the ultimate limit state. With respect to the concrete girder, it is proposed that no cracking may occur (or: cracks remain closed) for $q_p + 1/3q_q$. For a cable geometry according to figure 8a this condition resulted in two prestressing elements with $A_p \simeq 2*600 = 1200$ mm². Of course, the engineer may choose any other load combination corresponding to the instant of cracking.

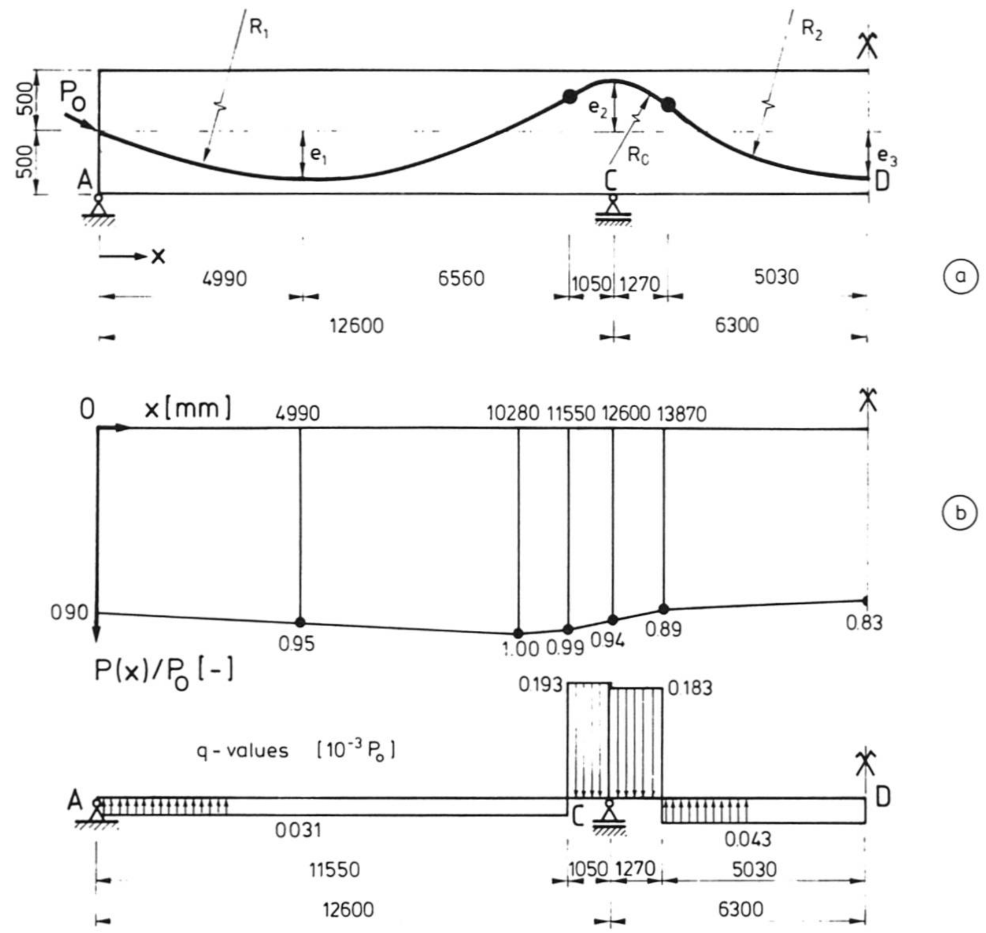

Fig. 8 (a) Prestressing tendon profile and (b) equivalent distributed and concentrated loading by prestress.

The required amounts of reinforcing steel A_s were determined to ensure the safety requirements. Next, the crack widths were checked: at C, a surplus of seven 20mm diameter bars was needed, which is a reduction of 68% in comparison with the reinforced concrete girder. See table 1 and figure 9.

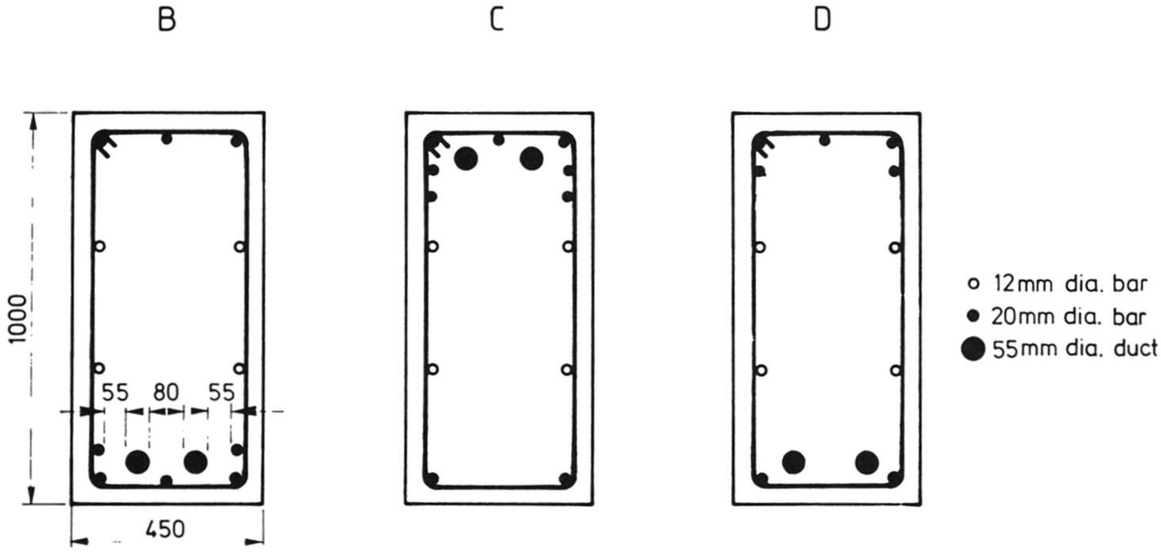

Fig. 9 Reinforcement for the cross-sections B, C and D respectively for 0.0 < K < 1.0.

With respect to the calculated crack widths, a factor c = 0.40 was implemented in eq. (3) taking account of the lower bond capacity of the post-tensioned prestressing strands [9]. The empirical formula for the crack spacing presented in [13] was adapted to cope with the effect of prestressing steel:

$$\Delta l_m = 50 + k_2 \cdot \frac{A_{c,eff} \cdot f_{ct}}{\Sigma u_s \tau_s + \Sigma u_p \tau_p} \qquad [mm] \qquad (6a)$$

In case of reinforced concrete $\Sigma u_p = 0$; $f_{ct} / \Sigma u_s = k_1$; $\Sigma u_s = n\pi d_s$ and $A_{c,eff} = n\pi d_s^2 / (4\rho_{eff})$ which yields eq. (6a):

$$\Delta l_m = 50 + \frac{k_2 . k_1 . d_s}{4\rho_{eff}} \qquad [mm] \qquad (6b)$$

ρ_{eff} is calculated in accordance with various national codes [8,13]. For one prestressing element the effective cross-sectional area has a maximum of 300*300 mm² [10,13,21]. Finally, τ_p and u_p are quantified according to [9,10]:

$$\tau_p = c . \tau_s \qquad [MPa] \qquad (6c)$$

$$u_p = 1.4\pi \sqrt{4A_p / \pi} \simeq 5 \sqrt{A_p} \qquad [mm] \qquad (6d)$$

After satisfying the demands with regard to rotational capacity and crack width limitation, the safety of the ultimate limit state was checked. It was found that $\gamma = 1.9$ at B (midspan) and 1.8 at C (support). Table 2 shows the degree of prestressing for three cross-sections: K is at least 0.57.

Table 2 Overview of K according to eq. (1)

cross-section	K [-]
B	0.58
C	0.57
D(⌣)	0.77

Vertical stirrups of 12mm diameter and 300mm spacing are used throughout the complete structure, which is considerably lower than in the case of a reinforced concrete structure because of the favourable effects of the distributed equivalent prestress loading. The tension zones of the girder all meet automatically the requirements of eqs. (4a)-(4b).

3.5 Level of prestress and economy

In the sections 3.1-3.4 it is shown that a continuous girder can be designed for different levels of prestress. The economic consequences of the level chosen have not yet been studied. Therefore, the costs of materials (reinforcing and prestressing steel) and labour (preparation and adjustment of the reinforcement, prestressing of the strands, grouting, etcetera) were estimated according to guide-lines presented by the Dutch building-industry (dated March 1987, prices excl. VAT in case of the manufacturing of at least ten continuous beams). An overview is shown in figure 10 for one girder. The results should be interpreted carefully as they partly depend on the specific example chosen.

Compared with the reinforced concrete girder, the partly prestressed beam offers a few advantages:
- The percentage of labour cost related to the reinforcing steel is reduced from 46% to 21% and the total duration of the work at the site may decrease;
- The total amount of reinforcement is reduced by 57% to about 72 kg steel bars per m³ of concrete.

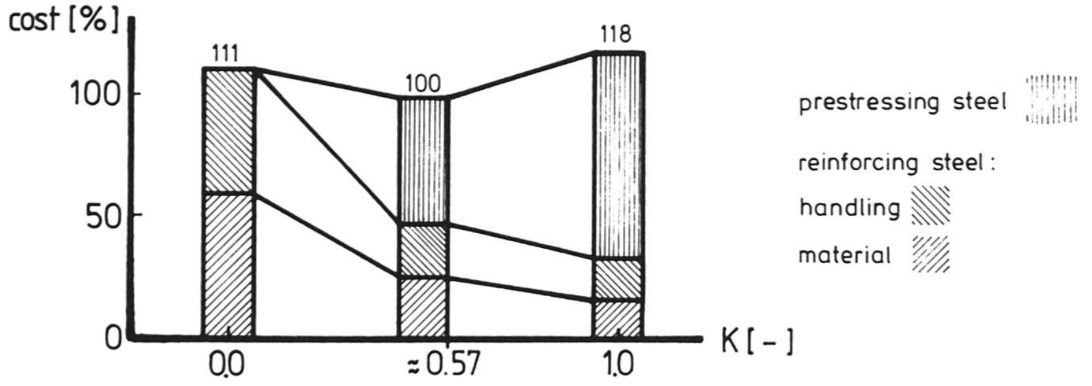

Fig. 10 Calculated distribution of reinforcement cost for three levels of prestress (100% ≃ dfl. 5200,- ≃ US$ 2500,- dated Oct. 1988).

4. DESIGN OF A STATICALLY INDETERMINATE BOX-GIRDER BRIDGE IN PARTIALLY PRESTRESSED CONCRETE

4.1 Introduction

The example shown in chapter 3 concerns an illustration of a simple calculation method for structural concrete which has been specified in chapter 2. Chapter 4 mainly deals with the non-linear analysis of a continuous 50m span box-girder bridge with 2*2 traffic lanes, subjected to dynamic traffic load. The bridge is a part of a motorway, see figure 11. The design live load consists of:
- two distributed line loads of 9 kN/m each;
- one 600 kN heavy-truck traffic load distributed over three axes.

Load transfer of the box-girder is only considered in the longitudinal direction of one span which is part of a long statically indeterminate structure. Material properties: f_{ccylk}= 36 MPa; f_{sy}= 400 MPa and f_{pk}= 1770 MPa.

Each of the three webs of the box-girder contains six prestressing elements of eight 15.3mm (5/8 inch) diameter strands so that A_p = 3*6*1120 = 20160 mm². See also figure 12. At the support A_s = 44400 mm² (upper-flange) and at the midspan A_s = 33000 mm² (lower-flange). These values grant that sufficiently small crack widths (see section 3.1) can be expected. The bending moments related to the serviceability and the ultimate limit states (see figure 3) are presented in table 3.

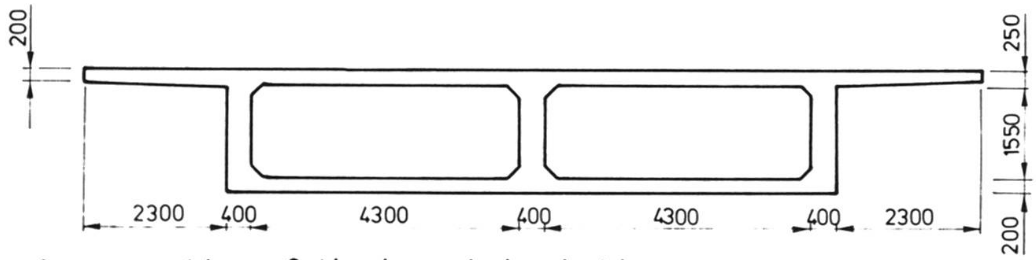

Fig. 11 Cross-section of the box-girder bridge.

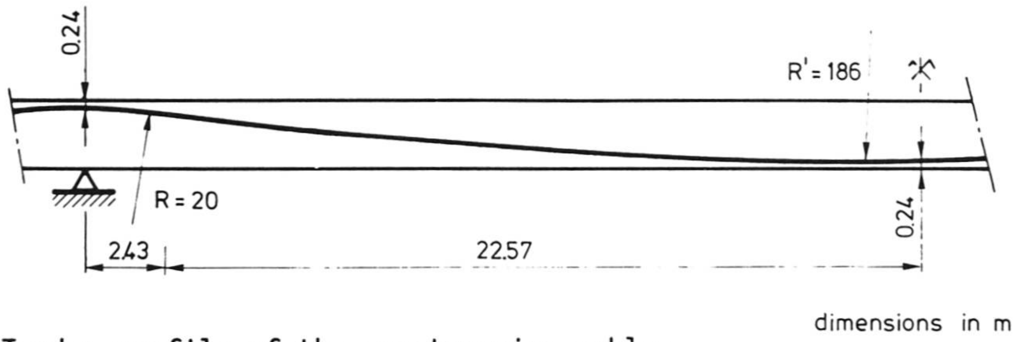

Fig. 12 Tendon profile of the prestressing cables.

Table 3 Overview of some calculated bending moments and the corresponding structural safety factors.

cross-section	M_{max} [kNm] d	M_{max} [kNm] d + l *)	M_u [kNm]	γ [-]
support (∩)	-44300	-56500	-98400	1.7
midspan (∪)	22100	34600	78100	2.3

*) d = dead load l = live load

4.2 Development of cracks

The average crack widths have been calculated in two ways. A first approximation is based on an assumed cooperation of reinforcing and prestressing steel leading to a uniform cracking pattern in the cross-sectional area of the concrete structure. A second approach takes account of a concentrated location of the prestressing elements at the flange-web connection of the box-girder, causing a distributed cracking pattern.
The average and the characteristic (95% upper-bound value) crack widths are respectively [8,13,15]:

$$w_m = \Delta l_m \cdot \epsilon_{sm} = \Delta l_m \cdot (\epsilon_s - \beta \Delta \epsilon_s) \qquad [mm] \qquad (7a)$$

$$w_k = 1.7 w_m \qquad [mm] \qquad (7b)$$

where β is a coefficient incorporating reduced tension-stiffening ($\Delta\epsilon_s$) by a dynamic or a sustained loading. A sensitivity analysis was carried out using β = 0.0, 0.5 and 1.0. From experimental and theoretical research [22] it was found that β = 0.5 fits closely to the actual structural behaviour [8,13]. The values in the tables 4 and 5 indicate that the permissible crack widths (section 3.1) are not exceeded.

Table 4 Predicted average crack widths in case of a uniform crack pattern.

cross-section	w_m [mm] at M_{max} β = 0.0	0.5	1.0
support	0.12	0.10	0.08
midspan	0.13	0.10	0.07

Table 5 Predicted average crack widths in case of a distributed crack pattern.

cross-section	prestressing steel			reinforcing steel		
	β = 0.0	0.5	1.0	0.0	0.5	1.0
support	0.11	0.10	0.08	0.13	0.10	0.08
midspan	0.08	0.07	0.06	0.11	0.09	0.07

4.3 Effect of steel stress variations

The last few years much research effort focused on the fatigue behaviour of reinforcing steel [23] and prestressing elements [24]. In-situ measurements of the dynamic traffic loading were carried out on structural concrete bridges [25]. Structural fatigue-failure of the reinforcement is related to an assumed percentage of 40% of the live load which should be exceeded by two million loading cycles during a 100-year life-time [26].
Further experimental research is needed, especially regarding realistic spectra of the traffic loadings, which should provide a more reliable percentage. Moreover, the gradual deterioration of the material during the fatigue process should be better quantified [34].
So far, the permissible stress-amplitudes still have an empirical background [21,27]:

$$\Delta\sigma_p = 104 \text{ MPa (prestressing strands)} \tag{8a}$$

$$\Delta\sigma_s = 180 \text{ MPa (reinforcing bars)} \tag{8b}$$

for steel grades f_{sy}= 400 MPa and f_{pk}= 1770 MPa, respectively [19].

The steel stress variations $\Delta\sigma_p$ should be multiplied by a factor c denoting the reduced bond characteristics of prestressing steel. Table 6 refers to a variation of the complete live load so that the stress-values are relatively high.

Table 6 Stress-variations in reinforcing and prestressing steel.

load variation	$\Delta\sigma_s$ [MPa] S *)	M **)	$\Delta\sigma_p$ [MPa] S	M
± 0.4 live load	50	30	20	20
± 1.0 live load	130	120	50	70

*) support **) midspan

4.4 Finite element analysis

The finite element program 'DIANA' was used in order to study the detailed structural behaviour of the box-girder bridge. 'DIANA' [28] takes account of non-linear material characteristics, such as cracking of concrete, multiaxial concrete strength envelopes (figure 13a), plasticity of the reinforcing and the prestressing elements (figure 13b) and tension-stiffening. The program uses the so-called smeared crack approach [29].

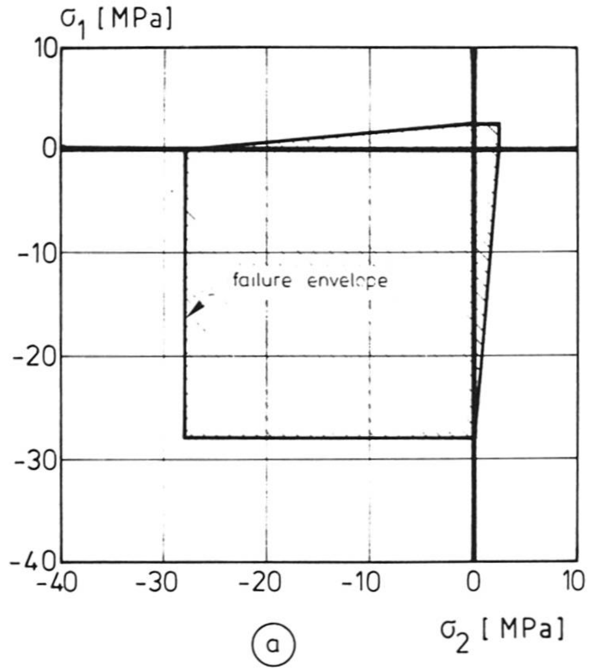

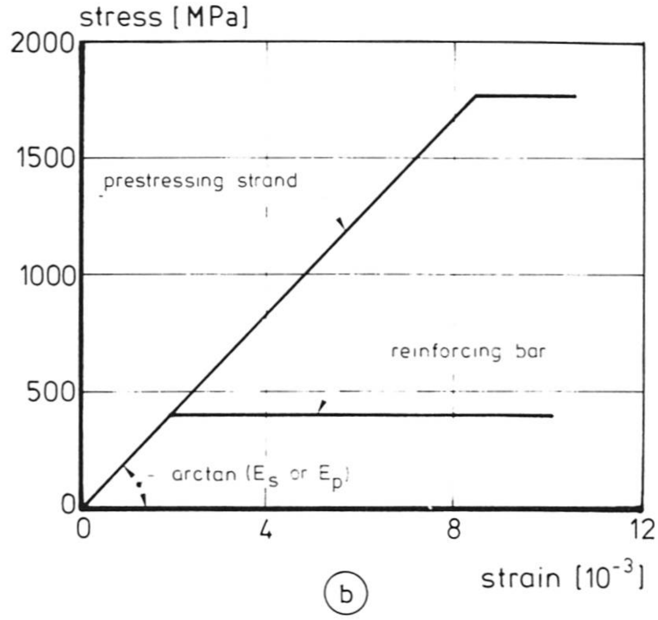

Fig. 13 Assumed models in 'DIANA' for (a) multiaxial concrete strength and (b) stress-strain diagrams of reinforcement.

A two-dimensional finite element mesh was taken for the box-girder bridge consisting of eight node plane stress elements, each with nine integration points. Figure 14 shows that the girder is modelled as a cantilever on account of symmetry. Perfect bond was assumed for the modelling of the reinforcing and the prestressing steel. The effective prestress loading was applied as an external load (figure 15) and the 'yield stress' was referred to the initial level of prestress. A uniformly distributed load - almost equivalent to the design load given in section 4.1 - was gradually increased during the computational simulation. The maximum load of 535 kN/m was reached due to compressive failure of the concrete at the support for ϵ_{cu}= -0.0035 and q_q= 212 kN/m.

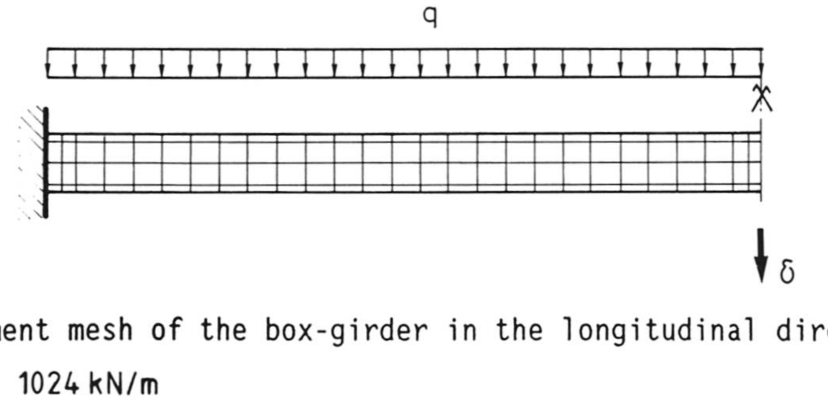

Fig. 14 Element mesh of the box-girder in the longitudinal direction.

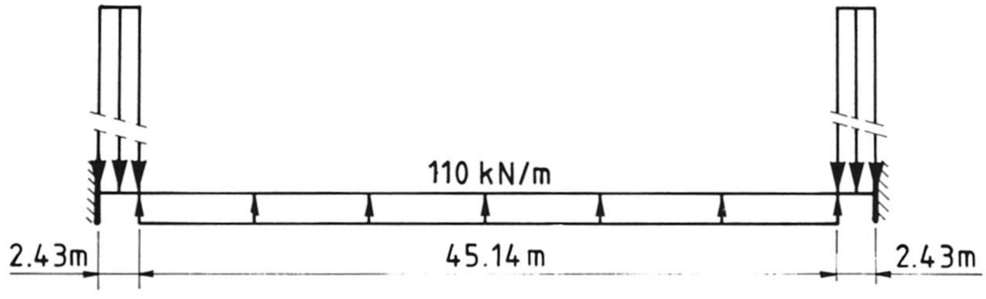

Fig. 15 Equivalent distributed prestress loading applied on the box-girder.

A few results are reviewed now:
- The load-deflection diagram of the midspan is shown in figure 16 and it closely agreed with a simple calculation method according to chapter 2;
- The longitudinal moment distribution as computed by 'DIANA' was compared with a simple linear elastic approximation based on a fully uncracked girder. Although considerable cracks occur at the serviceability limit state, the differences were less than 5%. At the ultimate limit state $M_u = -108900.10^6$ (support) and 60200.10^6 Nmm (midspan) according to 'DIANA';
- The bending moment at the support exceeds the value of section 4.3 with 10% which might be caused by the rather limited number of elements chosen in order to reduce the CPU-time. For instance, the height of the compression zone of the flanges is equal to the element size;
- Finally, figure 17 shows the crack pattern computed at the very instant of structural failure of the girder. The cracks are indicated as dashes located at the integration points of the elements. The dash length is proportional to the predicted crack strain. The computer simulations provide a clear insight into the actual structural behaviour.

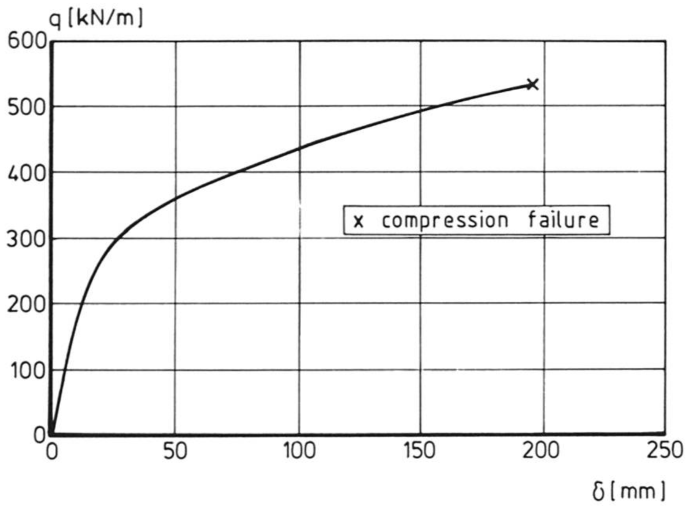

Fig. 16 Computed load-deflection diagram of the cross-section at midspan.

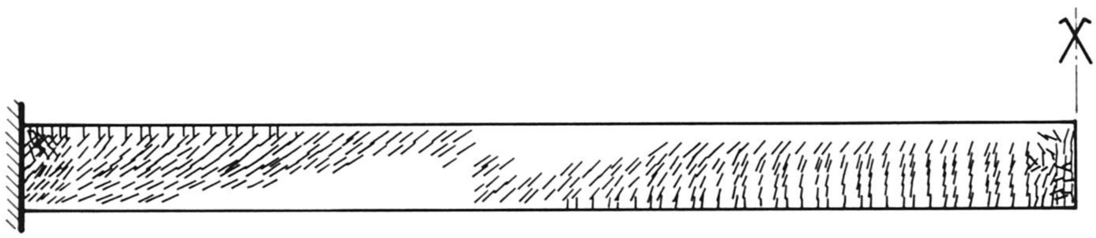

Fig. 17 Crack pattern of the box-girder according to 'DIANA'.

5. CONCLUSIONS AND RECOMMENDATIONS

The proposed simple calculation method has been applied to two statically indeterminate concrete structures, of which the cross-section is either a rectangle or a box-girder. Both design examples focused on partially prestressed concrete. Satisfactory results were achieved in comparison with reinforced concrete:
- reduced crack widths and deflections;
- more simple detailing of the reinforcement.

Partially prestressed concrete structures may often be advantageous if the ratio of live to dead load is relatively high or in case of a limited structural height. The computational results expose close agreement with a non-linear finite element analysis of the box-girder bridge. Apart from the technical point of view, partially prestressed concrete may exhibit good economic prospects, see section 3.5. Extended theoretical and experimental research is needed particularly with respect to the determination of crack widths in partially prestressed high-strength concrete [30].

6. NOTATION

Unless otherwise stated, the dimensions are N, mm or MPa. Dimensions in the figures are usually in mm.

$A_{c,eff}$ - effective cross-sectional area of cracked concrete [mm^2]
A_p - cross-sectional area of prestressing steel [mm^2]
A_s - cross-sectional area of reinforcing steel [mm^2]
b - cross-sectional width
c - bond factor of prestressing steel [-] or concrete cover
d - bar diameter or effective beam depth
e - eccentricity of prestressing cable
f_{cck} - characteristic cube compressive strength of concrete
f_{ccylk} - characteristic cylinder compressive strength of concrete
f_{ct} - pure tensile strength of concrete
$f_{ct,fl}$ - flexural tensile strength of concrete
f_{pk} - characteristic tensile strength of prestressing steel
f_{sy} - yield stress of reinforcing steel
h - height of structure
h_x - height of compression zone
h_t - height of tension zone
K - degree of prestressing [-]
M_{cr} - cracking moment of a cross-section [Nmm]
M_o - decompression moment of a cross-section [Nmm]
M_p - bending moment due to prestressing [Nmm]
M_u - ultimate moment of a cross-section [Nmm]
P - prestressing force
q_p - uniformly distributed dead load [N/mm]
q_q - uniformly distributed live load [N/mm]
R - radius of the centre line of curved tendons
u - circumference
V - shear force at a cross-section
w - crack width
β - reduction coefficient for tension-stiffening [-]
γ - coefficient of structural safety [-]
δ - deflection
$\epsilon_{s,m}$ - mean steel strain [-]
Δl_m - mean crack spacing
$\Delta\epsilon_s$ - steel strain reduction due to tension-stiffening [-]
$\Delta\sigma$ - stress variation due to dynamic loading
$\Delta\sigma_{s,cr}$ - stress increase of the reinforcing steel at the instant of cracking
σ_{po} - initial prestress
$\sigma_{p\infty}$ - effective prestress
τ_s - bond stress parallel to a deformed bar
ρ_d - reinforcement ratio (= $A_s/(bd)$)

7. REFERENCES

1. Cohn, M.Z., et al.:
"Partial prestressing, from theory to practice", NATO ASI Series, 1986, pp. 405 + 426.
2. Bachmann, H.:
"Partial prestressing of concrete structures", IABSE Periodica, No. S-11/79, Nov. 1979, 20 pp.
3. Bachmann, H.:
"Design of partially prestressed concrete structures based on Swiss experiences", PCI journal, vol. 29, no. 4, 1984, pp. 84-105.
4. Kupfer, H., et al.:
"Teilweise Vorspannung", Ernst & Sohn, Berlin, 1986, 250 pp.
5. Bruggeling, A.S.G.:
"Structural concrete: science into practice", Heron, vol. 32, no. 2, 1987, 67 pp.
6. Naaman, A.E., Siriaksorn, A.:
"Serviceability based design of partially prestressed beams", PCI journal, vol. 24, nos. 2/3, 1972, pp. 64-89 and 40-60.
7. Cohn, M.Z., Machae, A.J.:
"Prestressing optimization and its implications for design", PCI journal, vol. 29, no. 4, 1984, pp. 68-83.
8. CEB-FIP:
"Model Code for Concrete Structures", Bulletin d'information no. 124/125, 1978, 348 pp.
9. Thormählen, U.:
"Zum Einfluss von Spanngliedern mit nachträglichem Verbund auf Rissbildung und Rissbreitenbeschränkung bei teilweise vorgespannten Konstruktionen", T.H. Aachen, Dissertation, 1978, 199 pp. + Anlage.
10. Cordes, H., et al.:
"Teilweise Vorspannung; Verbundfestigkeit von Spanngliedern und ihre Bedeutung für Rissbildung und Rissbreitenbeschränkung", Deutscher Ausschuss für Stahlbeton, Heft 310, 1980, 140 pp.
11. Noakowski, P.:
"Verbundorientierte, kontinuierliche Theorie zur Ermittlung der Rissbreite", Beton- und Stahlbetonbau, vol. 80, nos. 7/8, 1985, pp. 185-190, 215-221.
12. Krips, M.:
"Rissbreitenbeschränkung im Stahlbeton und Spannbeton", T.H. Darmstadt, Heft 33, 1985, 155 pp.
13. Eurocode No. 2:
"Common unified rules for concrete structures", Draft, April 1988.
14. Martin, H., et al.:
"Berechnungsverfahren für Rissbreiten aus Lastbeanspruchung", Strassenbau und Strassenverkehrstechnik, Heft 309, 1980, pp. 33-66.
15. Schiessl, P., Wölfel, E.:
"Konstruktionsregeln zur Beschränkung der Rissbreite", Beton- und Stahlbetonbau, vol. 81, no. 1, 1986, pp. 8-15.
16. Fehling, E., König, G.:
"Crack width control and tension-stiffening", Darmstadt Concrete, T.H. Darmstadt, vol. 1, 1986, pp. 65-86.
17. Leonhardt, F., et al.:
"Vorlesungen über Massivbau, fünfter Teil: Spannbeton", Springer-Verlag, 1980, 296 pp.

18. Walraven, J.C.:
"Spannbeton", Technische Hochschule Darmstadt, 1988, 242 pp.
19. NEN 3880:
"Design code for concrete (in Dutch), VB 1974/1984", parts A-K, NNI, Delft, 1984, 523 pp.
20. Schiessl, P.:
"Einfluss von Rissen auf die Dauerhaftigkeit von Stahlbeton- und Spannbetonbauteilen", Deutscher Aussch. für Stahlb., Heft 370, 1986, pp. 9-52.
21. "Spannbeton - DIN 4227", Betonkalender, Teil 2, 1988, pp. 188-240.
22. Rohling, A.:
"Zum Einfluss des Verbundkriechens auf die Rissbreitenentwicklung sowie auf die Mitwirkung des Betons zwischen den Rissen", T.U. Braunschweig, Dissertation, 1987, 230 pp.
23. Charlier, H., et al.:
"Dynamische Probleme im Stahlbetonbau; Teil I: Der Baustoff Stahlbeton unter dynamischer Beanspruchung", Deutscher Ausschuss für Stahlbeton, Heft 342, 1983, pp. 1-130.
24. Müller, H.H.:
"Dauerschwingfestigkeit von Spanngliedern", Betonwerk + Fertigteil-Technik, vol. 52, no. 12, 1986, pp. 804-808.
25. Mayer, M.:
"Dauerfestigkeit von Spannbetonbauteilen", Deutscher Ausschuss für Stahlbeton, Heft 176, 1966, 69 pp.
26. Nürnberger, U.:
"Dauerschwingverhalten von Spannstählen", Bauingenieur, vol. 56, 1981, pp. 311-319.
27. "Beton und Stahlbeton, Bemessung und Ausführung - DIN 1045", Betonkalender, Teil 2, 1986, pp. 56-152.
28. Borst, R. de, et al.:
"DIANA, a three-dimensional, nonlinear finite element package on a microcomputer", Conference on 'Engineering software for microcomputers', Venice, 1984, pp. 435-446.
29. Rots, J.G.:
"Computational modeling of concrete fracture", Delft University of Technology, Dissertation, 1988, 132 pp.
30. Thorenfeldt, E., et al.:
"Mechanical properties of high-strength concrete and application in design", Symposium Utilization of high-strength concrete, Stavanger, June 1987, pp. 149-160.
31. Darwin, D.:
"Shear component of prestress by equivalent loads", PCI-journal, March/April 1977, pp. 64-77.
32. Braam, C.R., Frénay, J.W.:
"Working example of a statically indeterminate concrete girder" (in Dutch) Delft University of Technology, Fac. of Civil Eng., 1988, 41 pp.
33. Norm SIA 162:
"Norm für die Berechnung, Konstruktion and Ausführung von Bauwerken aus Beton, Stahlbeton und Spannbeton", Schweizerischer Ingenieur- und Architektenverein, Zürich, 1968, 81 pp.
34. Miner, M.A.:
"Cumulative damage in fatigue", Journal of applied mechanics, 1945, no. 12.
35. Frénay, J.W.:
"Time-dependent shear transfer in cracked reinforced concrete", Delft University of Technology, Dissertation, (to be published in 1989), 183 pp.